Scientific paper

Synthesis, Crystal Structure and Separation Performance of *p-tert*-butyl(tetradecyloxy)calix[6]arene

Wei Zhang,¹ Zhi-qiang Cai,^{1,*} Xiao-min Shuai,¹ Wei Li,¹ Qiu-chen Huang,¹ Ruo-nan Chen,¹ Qi-qi Zang,² Fei-fei Li² and Tao Sun^{2,*}

¹ Liaoning Province Professional and Technical Innovation Center for Fine Chemical Engineering of Aromatics Downstream, School of Petrochemical Engineering, Shenyang University of Technology, Liaoyang 111003, P. R. China.

² College of Chemistry and Chemical Engineering, Henan Key Laboratory of Function-Oriented Porous Materials, Luoyang Normal University, Luoyang 471934, P. R. China.

* Corresponding author: E-mail: kahongzqc@163.com; E-mail: suntao2226@163.com

Received: 10-19-2021

Abstract

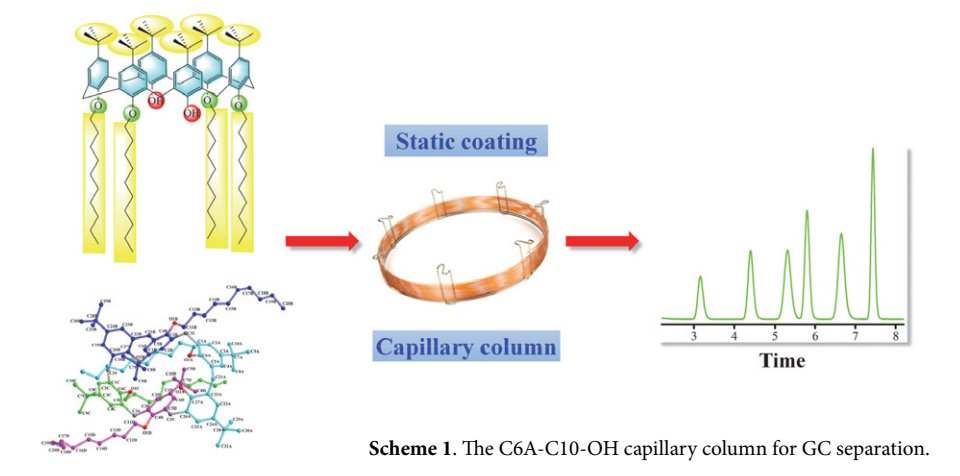
This work describes the investigation of separation performance of the p-tert-butyl(tetradecyloxy)calix[6]arene (C6A-C10-OH) as stationary phase for gas chromatography (GC) separations. Its structure was characterized by IR, 1 H NMR, 13 C NMR, MS and single-crystal X-ray diffraction analysis. The C6A-C10-OH column shows good separation capacity for aliphatic, aromatic and cis-/trans- isomers. Especially, it exhibits multiple molecular recognition interactions for the analytes with a wide range of polarity, including dispersion, π - π , H-bonding and dipole-dipole interactions. The present work provides experimental and theoretical basis for the designing of the new calixarene stationary phases in GC analyses.

Keywords: Calixarene; crystal structure; separation performance

1. Introduction

Calixarenes are the third generation of supramolecular compound after crown ethers and cyclodextrins.¹ These macrocyclic compounds have attracted extensive attention in the field of separation science because of it has unique physicochemical properties such as adjustable cavity size, good solubility, structural stability and so on.²

Their hydrophobic cavities are composed of benzene ring units, and its upper and lower rims are *p-tert*-butyls and phenolic hydroxyl groups, respectively, which are easy to derivatize.³ In recent years, calixarene derivatives with diverse structures have been widely used in various fields, such as catalysis, molecular recognition, energy and separation analysis.⁴



Zhang et al.: Synthesis, Crystal Structure and Separation Performance .

GC has widely applied in many fields including environmental analysis, petrochemical industry, food analysis and pharmaceutical analysis due to its excellent characteristics such as good selectivity, high sensitivity, rapid analysis and low cost.⁵ In GC, it is the key to choose a suitable stationary phase for the separation of compounds with close nature. In recent years, our group has been engaged in the research of new calixarene chromatographic stationary phases. In 2019, we first reported the amphiphilic calixarene (C4A-NH₂) and used it to separate aromatic amine isomers.⁶ Subsequently, we reported the study of calix[6]arene and calix[8]arene derivatives as stationary phases for GC.⁷ These results indicated that calixarenes and their derivatives are suitable as GC stationary phases with good chromatographic selectivity.

First, we synthesized a new calixarene compound (C6A-C10-OH) in this work. The upper rim is *p-tert*-butyl, and the lower rim is long alkyl chain and phenolic hydroxyl. Second, we characterized the molecular structure of C6A-C10-OH by IR, ¹H NMR, ¹³C NMR, MS and single-crystal X-ray diffraction analysis. Then, it was coated on the inner wall of capillary column by static method, and its chromatographic separation performance was investigated (Scheme 1).

2. Experimental

2. 1. Materials and Methods

An Agilent 7890A gas chromatograph was used for GC analyses. Thin layer chromatography (TLC) was performed on silica-gel plates (HF₂₅₄). 1 H NMR spectrum and 13 C NMR spectrum used TMS (tetramethylsilane) as the internal standard and exported on a Bruker BioSpin 400 MHz instrument. Chemical shifts (δ) were expressed in ppm. IR spectrum was reported on a Bruker Platinum ART Tensor II FTIR spectrometer. MALDI-TOF-MS was reported on a Bruker BIFLEX III mass spectrometer. Single Crystal data of C6A-C10-OH were gained on a Bruker D8 VENTURE X-ray diffractometer. All reagents and solvents were not further treated, and all from commercial way.

2. 2. Synthesis of the C6A-C10-OH

Firstly, NaH (1.24 g, 51.67 mmol), *p-tert*-butylcalix[6] arene (1.50 g, 1.54 mmol) and DMF (25 mL) were added to a 50 mL round bottom flask. The reactants were reacted at room temperature for 1 h. Afterwards, 1-bromodecane (4.30 g, 19.19 mmol) was added to mixed solution, raised the temperature to 85 °C and reacted for 10 h. After the reaction, the solvent was concentrated to obtain a yellow solid. Then, dichloromethane was used to dissolve the obtained yellow solid and rinsed three times with deionized water (15 mL). Then, the anhydrous magnesium sulfate was used to remove water and vacuum drying. Fi-

nally, a light yellow oily product was obtained. Using column chromatography [dichloromethane/petroleum ether (v/v=1:4)] to purify the product of the previous step, and the final white solid product was gained with a yield of 85.34%. ¹H NMR (400 MHz, CDCl₃, ppm): δ 7.39 (s, 4H, CH), 7.04 (s, 8H, CH), 4.05 (m,8H, CH₂), 3.84 (s, 12H, CH₂), 1.60 (m, 8H, CH₂), 1.42 (m, 8H, CH₂), 1.27 (s, 54H, CH₃), 1.22 (m, 48H, CH₂), 0.86 (t,12H, CH₃); ¹³C NMR (100 MHz, CDCl₃, ppm): δ 151.57, 151.15, 146.93, 142.79, 132.78, 126.23, 125.70, 77.48, 77.16, 76.84, 34.29–33.67, 32.19–31.90, 31.90–30.69, 30.16–29.01, 26.50, 23.05–22.74, 14.29; IR (KBr), cm⁻¹: v(OH) 3373, v(CH₃) 2955, v(CH₂) 2929, v(CH₂) 2858, v(C=C) 1484, v(C=C) 1460, v(C-O-C) 1188, v(CH₂) 722; ESI-MS(m/z): [M+K]⁺calcd for C₁₀₆H₁₆₄O₆, 1572.253; found, 1572.166.

2. 3. X-Ray Structure Determination

Took a small amount of white solid of the C6A-C10-OH and dissolved it in dichloromethane. After two days, dichloromethane volatilizes completely, we gained the white crystal for single crystal diffraction analysis. The dimensions of white crystal ($C_{106}H_{164}O_6$) were 0.17mm × 0.12mm × 0.12mm, and which were measured on a Bruker D8 VENTURE diffractometer equipped with graphite-monochromatic Mo $K\alpha$ radiation (λ = 1.54178 Å) using an ω scan mode at 103(2) K. A total of 55912 reflections were gathered in the range of 2.457° < θ < 70.168° (index ranges: $-12 \le h \le 12$, $-43 \le k \le 42$ and $-30 \le l \le 30$) and 17547 were independent ($R_{\rm int}$ = 0.0745), of which 11531 observed reflections with $I > 2\sigma(I)$ were applied in the refinements and structure determination. Used the intrinsic phasing methods to confirm the structure with

Table 1. Crystal data of the C6A-C10-OH

$\begin{array}{llllllllllllllllllllllllllllllllllll$	Crystal size	$0.170 \times 0.120 \times 0.120 \text{ mm}^3$
$\begin{array}{llll} T \ (K) & 103(2) \ K \\ Crystal \ system & Monoclinic \\ Space \ group & Cc \\ a \ (\mathring{A}) & 10.5965(5) \\ b \ (\mathring{A}) & 35.9665(16) \\ c \ (\mathring{A}) & 25.1721(11) \\ \alpha \ (^{\circ}) & 90 \\ \beta \ (^{\circ}) & 92.663(3) \\ \gamma \ (^{\circ}) & 90 \\ V \ (\mathring{A})^3 & 9583.2(7) \\ Z & 4 \\ D_c \ (g/cm^3) & 1.063 \\ F(000) & 3392 \\ Goodness-of-fit \ on \ F^2 & 1.075 \\ Reflection \ collected & 55912 \\ R_1, \ wR_2 \ [I > 2\sigma \ (I)] & 0.0852, 0.2445 \\ \end{array}$	Formula	$C_{106}H_{164}O_6$
$\begin{array}{cccccccccccccccccccccccccccccccccccc$	Molecular weight	1534.36
$\begin{array}{llllllllllllllllllllllllllllllllllll$	T (K)	103(2) K
$\begin{array}{llllllllllllllllllllllllllllllllllll$	Crystal system	Monoclinic
$\begin{array}{llllllllllllllllllllllllllllllllllll$	Space group	Cc
$\begin{array}{cccc} c\ (\mathring{A}) & & & & & & \\ \alpha\ (^{\circ}) & & & & & \\ \beta\ (^{\circ}) & & & & \\ \beta\ (^{\circ}) & & & & \\ \gamma\ (^{\circ}) & & & \\ Y\ (\mathring{A})^3 & & \\ Y\ (\mathring{A})^3 & & \\ Y\ (\mathring{A})^3 & & \\ Y\ (\mathring{A})^3 & & & \\ Y\ (\mathring{A})^3 & & \\ Y\ (\mathring{A})^3 & & \\ Y\$	a (Å)	10.5965(5)
$\begin{array}{lll} \alpha (^{\circ}) & 90 \\ \beta (^{\circ}) & 92.663(3) \\ \gamma (^{\circ}) & 90 \\ V (\mathring{A})^3 & 9583.2(7) \\ Z & 4 \\ D_c (g/cm^3) & 1.063 \\ F(000) & 3392 \\ Goodness-of-fit on F^2 & 1.075 \\ Reflection collected & 55912 \\ R_1, wR_2 [I > 2\sigma (I)] & 0.0852, 0.2445 \\ \end{array}$	b (Å)	35.9665(16)
$\begin{array}{lll} \beta (^{\circ}) & & 92.663(3) \\ \gamma (^{\circ}) & & 90 \\ V (\mathring{A})^3 & & 9583.2(7) \\ Z & & 4 \\ D_c (g/cm^3) & & 1.063 \\ F(000) & & 3392 \\ Goodness-of-fit on F^2 & & 1.075 \\ Reflection collected & & 55912 \\ R_1, wR_2 [I > 2\sigma (I)] & & 0.0852, 0.2445 \\ \end{array}$	c (Å)	25.1721(11)
$\begin{array}{lll} \gamma^{(e)} & 90 \\ V^{(e)} & 9583.2(7) \\ Z & 4 \\ D_c^{(e)}(g/cm^3) & 1.063 \\ F(000) & 3392 \\ Goodness-of-fit on F^2 & 1.075 \\ Reflection collected & 55912 \\ R_1, wR_2^{[I]} = 2\sigma^{(I)} & 0.0852, 0.2445 \\ \end{array}$	α (°)	90
$\begin{array}{cccccccccccccccccccccccccccccccccccc$	β (°)	92.663(3)
$\begin{array}{cccc} Z & & 4 & & \\ D_c (g/cm^3) & & 1.063 & \\ F(000) & & 3392 & \\ Goodness-of-fit on F^2 & & 1.075 & \\ Reflection collected & & 55912 & \\ R_1, wR_2 [I > 2\sigma (I)] & & 0.0852, 0.2445 & \\ \end{array}$	γ (°)	90
$\begin{array}{cccc} D_c (g/cm^3) & 1.063 \\ F(000) & 3392 \\ Goodness-of-fit on F^2 & 1.075 \\ Reflection collected & 55912 \\ R_1, wR_2 [I > 2\sigma (I)] & 0.0852, 0.2445 \\ \end{array}$	$V (Å)^3$	9583.2(7)
$\begin{array}{lll} F(000) & 3392 \\ Goodness-of-fit on F^2 & 1.075 \\ Reflection collected & 55912 \\ R_1, wR_2 \ [I > 2\sigma \ (I)] & 0.0852, 0.2445 \end{array}$	Z	4
	$D_c(g/cm^3)$	1.063
Reflection collected 55912 R_1 , w R_2 [I > 2 σ (I)] 0.0852, 0.2445	F(000)	3392
R_1 , wR_2 [I > 2 σ (I)] 0.0852, 0.2445	Goodness-of-fit on F ²	1.075
1. 21 (7)	Reflection collected	55912
R ₁ , wR ₂ (all data) 0.1135, 0.2743	R_1 , $wR_2 [I > 2\sigma (I)]$	0.0852, 0.2445
	R ₁ , wR ₂ (all data)	0.1135, 0.2743

 $R_1 = \sum (||F_0| - |F_c||) / \sum |F_0| \dots w R_2 = (\sum w (F_0^2 - F_c^2)^2 / \sum w (F_0^2)^2)^{1/2}$

the SHELXT 2014 program and reported by the Fourier technique. The non-hydrogen atoms were purified anisotropically. Through theoretical calculation, we reached the hydrogen atom combined with carbon atom. The structure was purged by the full-matrix least-squares techniques on F^2 with SHELXL-2017. The final refinement gave R=0.0852 and wR=0.2743 ($w=1/[\sigma^2(F_o^2)+(P)^2+P)]$, where $P=(F_o^2+2F_c^2)/3$), S=1.075, $(\Delta/\sigma)_{\rm max}=0.002$, $(\Delta\rho)_{\rm max}=0.694$ and $(\Delta\rho)_{\rm min}=-0.278$ e/Å 3 . Other crystal structure data of C6A-C10-OH are shown in Table 1.

2. 4. Preparation of the Capillary Column

The static coating method was used to make the C6A-C10-OH capillary column.9 Firstly, the dichloromethane was used to rinse the empty column (0.25 mm × 10 m) to remove impurities. The rinsed capillary column was filled by a NaCl-MeOH saturated solution to rough inner wall of capillary column. Then, it was rised from 40 °C to 200 °C and maintained at 200 °C for 3 h. Next, the C6A-C10-OH stationary phase was dissolved in dichloromethane (2 mL) and injected into the treated column. When the column was completely full of stationary phase solution, sealed one end of the chromatographic column and connected the other end to the vacuum environment at 40 °C to evaporate the excess dichloromethane solution. Temperature process started at 40 °C hold for 30 minutes rise to 160 °C at the rate of 1 °C/min and maintained at 160 °C for 7 h. The experimental process was operated in nitrogen atmosphere.

3. Results and Discussion

3. 1. Synthesis and Characterization

Scheme 2 exhibits the synthetic process of C6A-C10-OH and it was obtained by one-step reaction. Meanwhile, IR, ¹H NMR, ¹³C NMR, MS and single-crystal X-ray diffraction analysis interpreted the molecular structure of C6A-C10-OH. In the IR, the peak value of 2955 cm⁻¹ was

C-H antisymmetric stretching vibration on the *p-tert*-butyl. The peak values of 1484 and 1460 cm⁻¹ was the C=C stretching vibration on benzene ring units. The peak value of 1188 cm⁻¹ was the C-O-C stretching vibration of ether, the peak value of 722 cm⁻¹ was the CH₂ plane rocking vibration of alkyl chains in the compound. In the $^1\mathrm{H}$ NMR, the proton absorption peaks of the aromatic rings were observed at 7.39 and 7.04 ppm in the low field, the proton absorption peaks of the bridged methylene in the benzene rings were discovered at 3.84 ppm, and the proton absorption peaks of methyl on *p-tert*-butyls and alkyl chains were found at 1.27 and 0.86 ppm, respectively. The integral area of each peak was consistent with the expected number of protons. Moreover, the structure of C6A-C10-OH was also characterized by $^{13}\mathrm{C}$ NMR.

3. 2. Crystal Structure of the C6A-C10-OH

Fig. 1 presents the molecular structure of the C6A-C10-OH, the crystal data and selected bond lengths are listed in the Table 1 and the Table 2 respectively. Its molecular structure consisted of six benzene rings, the four alkyl chains and two phenolic hydroxyl groups at the lower of C6A. The torsion angle of C(5)B-C(21)B-C(22)B-C(27) B was -90.0(8)°, which suggested that the two blue benzene rings were perpendicular to each other in space. The torsion angle of C(4)B-C(5)B-C(6)B-C(1)B was 0.1(10)°, which further proved that the carbon atoms on the benzene ring were coplanar. In the Table 2, the bond lengths of C(23)B-C(24)B (1.387(10) Å) and C(22)B-C(23)B (1.391(11) Å) were almost equal because these two bonds were in the same benzene ring. The bond length of O(1)B-C(11)B (1.416(9) Å) is shorter than C(11)B-C(12)B (1.519(11) Å). This is because the electronegativity of oxygen atom was larger than that of carbon atom, so that the bond energy of C=O was stronger than that of C=C. Moreover, Fig. 2 depicts the molecular packing in the unit cell and Table 3 gives that the hydrogen bond lengths and bond angles in the structure. 10

Scheme 2: Synthesis of the C6A-C10-OH

C6A-C10-OH

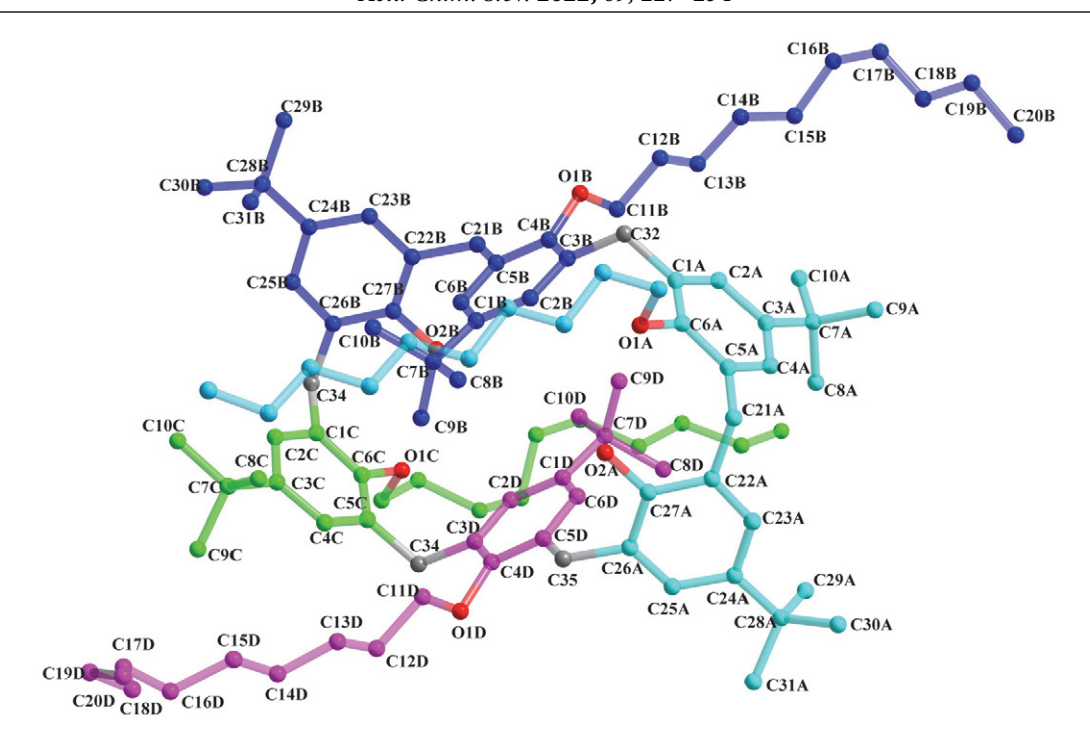
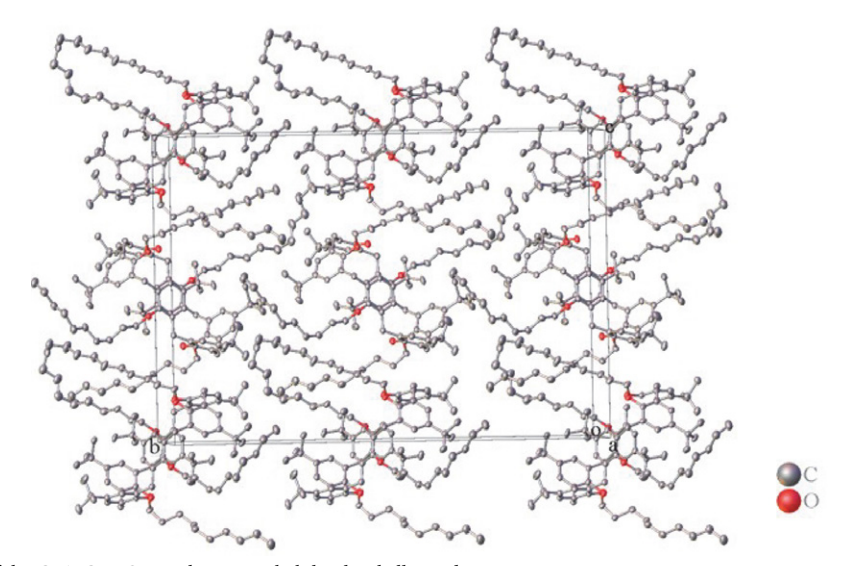


Fig. 1. Molecular structure of the C6A-C10-OH



 $\textbf{Fig. 2.} \ \ \text{Packing diagram of the C6A-C10-OH with 50\% probability level ellipsoids}$

Table 2. Selected Bond Lengths (Å) and Bond Angles (°) for the C6A-C10-OH

Bond	Dist.	Bond	Dist.	Bond	Dist.
C(28)B-C(29)B 1.515(1)		C(21)B-C(22)B	1.522(9)	O(1)B-C(11)B	1.416(9)
C(24)B-C(28)B	1.526(11)	C(5)B-C(21)B	1.531(11)	C(11)B-C(12)B	1.519(11)
C(23)B-C(24)B	1.387(10)	C(4)B-C(5)B	1.399(9)	C(12)B-C(13)B	1.544(11)
C(22)B-C(23)B	1.391(11)	O(1)B-C(4)B	1.409(9)	C(13)B-C(14)B	1.449(13)
Angle	(°)	Angle	(°)	Angle	(°)
C(29)B-C(28)B-C(24)B	111.7(7)	C(22)B-C(21)B-C(5)B	111.5(6)	O(1)B-C(11)B-C(12)B	106.5(6)
C(23)B-C(24)B-C(28)B	122.8(7)	C(4)B-C(5)B-C(21)B	120.0(6)	C(11)B-C(12)B-C(13)B	113.6(7)
C(24)B-C(23)B-C(22)B	123.3(7)	C(5)B-C(4)B-O(1)B	120.8(7)	C(14)B-C(13)B-C(12)B	113.7(8)
C(23)B-C(22)B-C(21)B	119.7(6)	C(4)B-O(1)B-C(11)B	117.6(6)	C(13)B-C(14)B-C(15)B	118.5(9)

Table 3. Hydrogen Bond Lengths (Å) and Bond Angles (°) for the C6A-C10-OH

D-HA	d(D-H)	d(HA)	d(DA)	<(DHA)
O(2)A-H(2)AO(1)A	0.84	2.08	2.891(8)	162.9
O(2)B-H(2)BO(1)C	0.84	2.04	2.874(7)	170.3

3. 3. Separation Performance of the C6A-C10-OH

The column efficiency of C6A-C10-OH column was 2400 plates/m. Afterwards, the aromatic and *cis-/trans*-isomers were used to study its separation performance.

The results shown that the C6A-C10-OH column achieved baseline resolution for above analytes.

Fig. 3 shows the separation of aromatic isomers of different polarity on the C6A-C10-OH column, such as substituted benzenes, trimethylbenzene and trichloroben-

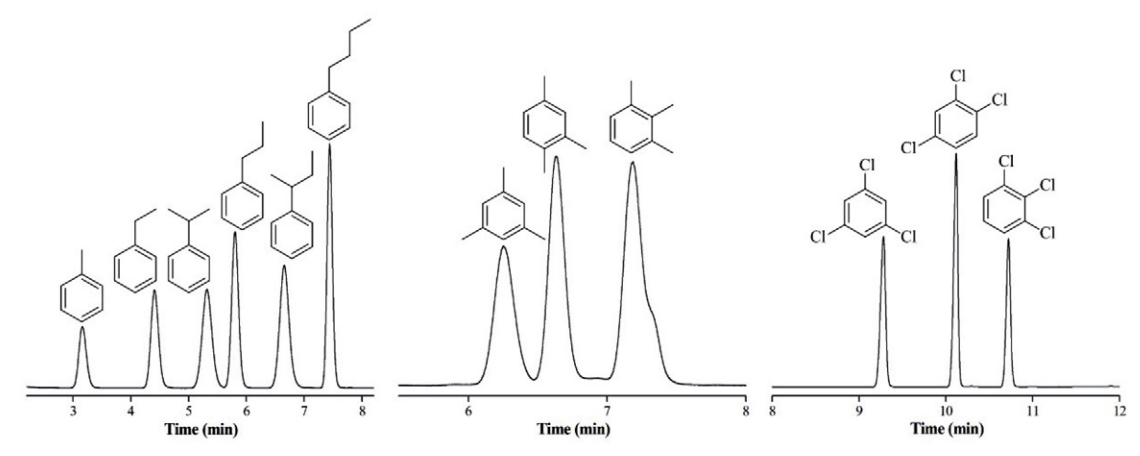


Fig. 3. GC separations of aromatic isomers. Temperature process: 40 °C (keep 1 min) up to 160 °C (keep 5 min) at 10 °C/min and gas flow rate at 0.6 mL/min.

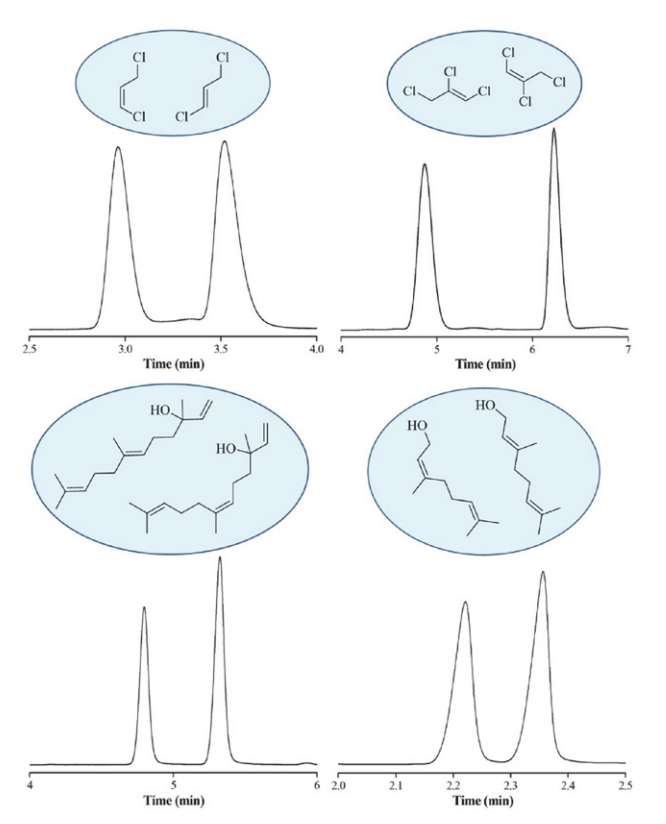


Fig. 4. GC separations of *cis-/trans-* isomers. Temperature process: 40 °C (keep 1 min) up to 160 °C (keep 5 min) at 10 °C/min and gas flow rate at 0.6 mL/min.

zene isomers. The C6A-C10-OH column presented excellent peak shapes for the benzene analytes and had a good resolution (R > 1.5). The C6A-C10-OH stationary phase had the good separation capacity for aromatic isomers due to its unique 3D cavity and aromatic framework, which can provide π - π interactions between stationary phase and aromatic analytes. In addition, *cis-/trans-* isomers were used to study the interaction mechanism between them in the C6A-C10-OH column.

Fig. 4 displays that the separations of *cis-/trans-* isomers on the C6A-C10-OH column, including 1,3-dichloropropene, 1,2,3-trichloropropene, nerolidol and nerol/geraniol. The results exhibited that the *cis-/trans-* isomers were well separated. It is worth to note that the C6A-C10-OH column had outstanding resolution for analytes with close boiling point, such as nerol (b.p. 226 °C)/geraniol (b.p. 229 °C), the boiling point difference was only 3 °C. This proved that the C6A-C10-OH column had excellent separation ability for the analytes of similar structure and physicochemical properties.

3. 4. Relationship Between Molecular Structure and Retention Behavior

In order to further study the relationship between molecular structure and retention behavior of the C6A-C10-OH stationary phase, we investigated its polarity and selectivity

in comparison to C6A-C10 stationary phase (the previous work of our group).⁷ The McReynolds constants of the C6A-C10-OH and C6A-C10 stationary phases were determined by the five probe compounds at 120 °C. Their sum and average values were used to characterize their general polarity and average polarity. In general, it can be regarded as non-po-

lar and moderately polar when the polarities of stationary phases are less than 100 and between 100 and 400 respectively. As shown in table 4, the average value of C6A-C10 stationary phase was 89, belonging to nonpolar, but the average value of C6A-C10-OH stationary phase was 129, indicating its moderate polarity. This polarity difference may derive

Table 4. McReynolds constants of the C6A-C10-OH and C6A-C10 columns

Stationary phases	X'	Y'	Z'	U'	S'	General polarity	Average
C6A-C10-OH	68	153	99	165	161	645	129
C6A-C10	41	124	73	115	92	445	89

X', benzene; Y', 1-butanol; Z', 2-pentanone; U', 1-nitropropane; S', pyridine. Temperature: 120 °C.

Table 5. The boiling point of alcohols and *n*-alkanes

Alcohols Compound	Molecular formula	Boiling point	n-Alkanes Compound	Molecular formula	Boiling point	
1-nonanol	C9H20O	215 °C	n-dodecane	C12H26	216 °C	
1-decanol	C10H22O	233 °C	<i>n</i> -tridecane	C13H28	235 °C	
1-undecanol	C11H24O	241 °C	<i>n</i> -tetradecane	C14H30	254 °C	
1-dodecanol	C12H26O	260 °C	<i>n</i> -pentadecane	C15H32	268 °C	

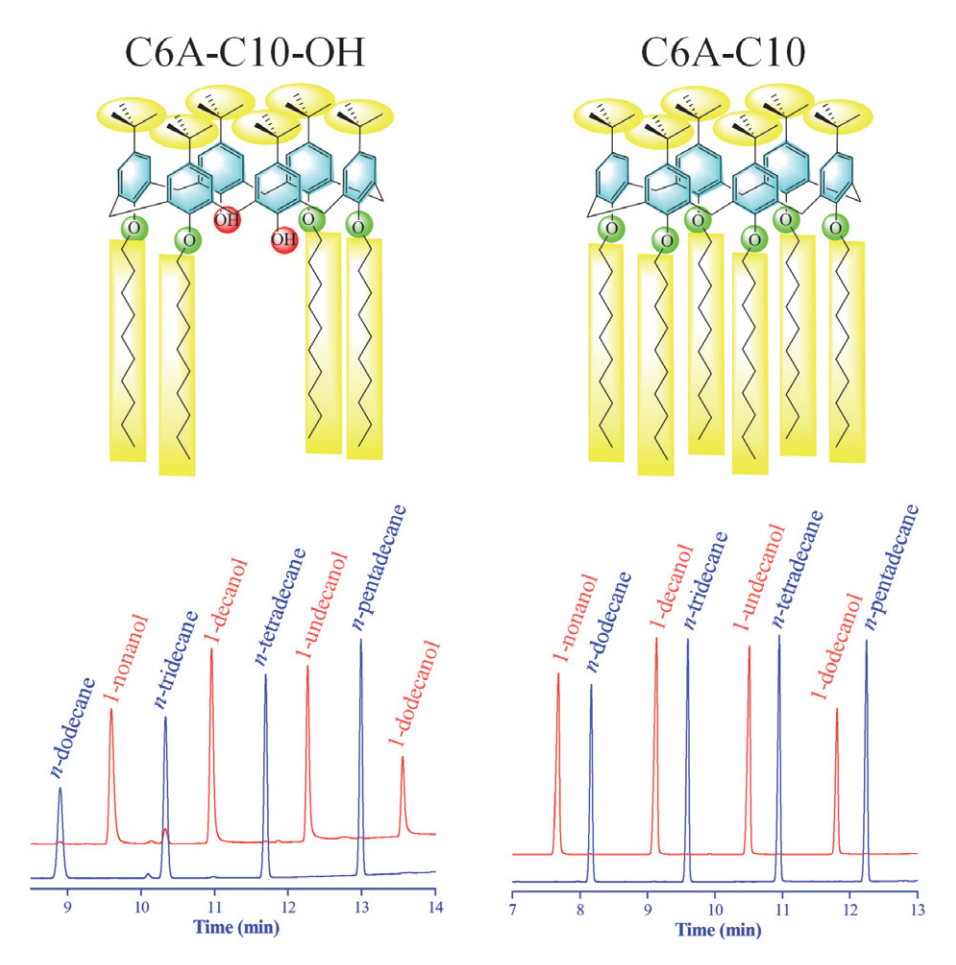


Fig. 5. GC separations of the alcohols and *n*-alkanes on the C6A-C10-OH and C6A-C10 columns. Temperature process: 40 °C (keep 1 min) up to 160 °C (keep 5 min) at 10 °C/min and gas flow rate at 0.6 mL/min.

from the different structures, the C6A-C10-OH stationary phase contained two unsubstituted phenolic hydroxyl groups, so its polarity was higher than C6A-C10 stationary phase and may offer H-bonding and dipole-dipole interactions for the separations of polar analytes.

Fig. 5 presents the separetions of the alcohols and *n*-alkanes on the C6A-C10-OH and C6A-C10 columns with the same separation conditions, respectively. The boiling points of analytes are listed in the Table 5. As shown, the C6A-C10-OH column exhibited the excellent resolving ability and good peak shapes for *n*-alkanes and alcohols. Interestingly, the C6A-C10-OH stationary phase exhibited stronger retention trend for the polar alcohols than the non-polar *n*-alkanes, such as the analyte pairs of *n*-dodecane/1-nonanol (b.p. 216 °C/b.p. 215 °C), *n*-tridecane/1-decanol (b.p. 235 °C/b.p. 233 °C), *n*-tetradecane/1-undecanol (b.p. 254 °C/b.p. 241 °C) and *n*-pentadecane/1-dodecanol (b.p. 268 °C/b.p. 260 °C).

However, the alcohols and alkanes were eluted in the order of boiling points on the C6A-C10 column. The above results showed that the retention behaviors of alcohols and alkanes in the two columns are quite different. This is because they have different molecular structures. C6A-C10-OH has two phenolic hydroxyl groups at the lower rim, so there are strong H-bonding and dipole-dipole interactions between the stationary phase and the polar analytes. The interactions between C6A-C10 and the linear analytes are mainly dispersion interactions, because the lower rim of its aromatic skeleton are all alkyl chain substituents. The above results proved that the C6A-C10-OH stationary phase had multiple molecular recognition interactions for different types of analytes due to its unique molecular structure, including dispersion, H-bonding and dipole-dipole interactions.

4. Conclusion

This work presents the investigation of the C6A-C10-OH stationary phase for GC separations. Its molecular structure was characterized by IR, ¹H NMR, ¹³C NMR, MS and single-crystal X-ray diffraction analysis. As demonstrated, the C6A-C10-OH stationary phase presents good separation capacity for aliphatic, aromatic and *cis-/trans-* isomers. Importantly, it exhibits prolonged retention trend for alcohols mainly due to the H-bonding and dipole-dipole interactions with the phenolic hydroxyl groups. In short, this work illustrates the outstanding separation ability of the C6A-C10-OH stationary phase for diverse analytes owing to its distinct molecular structure and multiple interactions.

Supplementary Material

CCDC 2093329 contains the supplementary data for this paper. The data can be obtained free of charge from

the Cambridge Crystallographic Data Centre via http://summary.ccdc.cam.ac.uk/structure-summary-form.

Acknowledgements

The authors thank the financial support of the Natural Science Foundation of Liaoning Province (20180550016) and the Scientific Research Foundation of the Education Department of Liaoning Province (LJGD2020015).

5. References

- S. Shinkai, *Tetrahedron*. 1993, 49, 8933–8968.
 DOI:10.1016/S0040-4020(01)91215-3
- (a) H. J. Kim, M. H. Lee, L. Mutihac, J. Vicens, J. S. Kim, Chem. Soc. Rev. 2012, 41, 1173–1190.

DOI:10.1039/C1CS15169J

- (b) C. Schneider, U. Menyes, T. Jira, *J. Sep. Sci.* **2010**, *33*, 2930–2942. **DOI**:10.1002/jssc.201000281
- (c) D. Guillaume, L. Roy, J. Ivan, A. Valerie, C. Pascal, *Curr. Org. Chem.* **2015**, *19*, 2237–2249.
- (a) N. Y. Edwards, A. L. Possanza, Supramol. Chem. 2013, 25, 446–463. DOI:10.1080/10610278.2013.794277
 - (b) N. Bregović, N. Cindro, L. Frkanec, V. Tomišić, *Supramol. Chem.* **2016**,28, 608–615.

DOI:10.1080/10610278.2016.1154147

- (c) S. E. Matthews, P. D. Beer, Supramol. Chem. **2005**, 17, 411–435. **DOI**:10.1080/10610270500127089
- (a) M. Schulz, A. Gehl, J. Schlenkrich, H. A. Schulze, S. Zimmermann, A. Schaate, *Angew. Chem. Int. Ed.* 2018, 57, 12961–12965. DOI:10.1002/anie.201805355
 - (b) K. Kurzątkowska, S. Sayin, M. Yilmaz, H. Radecka, J. Radecki, Sens. Actuators B Chem. 2015, 218, 111–121.

DOI:10.1016/j.snb.2015.04.110

(c) M. De Rosa, P. La Manna, A. Soriente, C. Gaeta, C. Talotta, P. Neri, *RSC Adv.* **2016**, *6*, 91846–91851.

DOI:10.1039/C6RA19270J

- (d) M.Yilmaz, S. Erdemir, *Turk. J. Chem.* **2013**, *37*, 558–585. **DOI**:10.3906/vet-1210-33
- (e) P. M. Mareeswaran, D. Maheshwaran, E. Babu, S. Rajagopal, *J Fluoresc.* **2012**, *22*, 1345–1356.

DOI:10.1007/s10895-012-1074-9

- (f) W. F. Zhang, Y. H. Zhang, Y. M. Zhang, C. Lan, Y. Miao, Z. F. Deng, X. Ba, W. D. Zhao, S. S. Zhang, *Talanta.* **2019**, *193*, 56–63. **DOI**:10.1016/j.talanta.2018.09.083
- (a) B. J. Pollo, G. L. Alexandrino, F. Augusto, L. W. Hantao, Trends Analyt. Chem. 2018, 105, 202–217.

DOI:10.1016/j.trac.2018.05.007

- (b) A. M. Muscalu, T. Górecki, *Trends Analyt. Chem.* **2018**, 106, 225–245. **DOI:**10.1016/j.trac.2018.07.001
- (c) M. V. Russo, P. Avino, L. Perugini, I. Notardonato, *RSC Adv.* **2015**, *5*, 37023–37043. **DOI:**10.1039/C5RA01916H
- (d) C. Citti, D. Braghiroli, M. A. Vandelli, G. Cannazza, J. *Pharmaceut. Biomed.* **2018**, *147*, 565–579.

DOI:10.1016/j.jpba.2017.06.003

- T. Sun, L. R. Qi, W. W. Li, Y. Li, X. M. Shuai, Z. Q. Cai, H. P. Chen, X. G. Qiao, L. F. Ma, *J. Chromatogr. A.* 2019, *1601*, 310–318. DOI:10.1016/j.chroma.2019.04.068
- (a)T. Sun, X. M. Shuai, Y. J. Chen, X. Y. Zhao, Q. Q. Song, K. X. Ren, X. X. Jiang, S. Q. Hu, Z. Q. Cai, RSC Adv. 2019, 9, 38486–38495. DOI:10.1039/C9RA07798G
 (b) X. M. Shuai, Z. Q. Cai, Y. J. Chen, X. Y. Zhao, Q. Q. Song, K. X. Ren, X. X. Jiang, T. Sun, S. Q. Hu, Microchem. J. 2020, 157, 105124. DOI:10.1016/j.microc.2020.105124
- G. M. Sheldrick, Acta Crystallogr A. 2015, 71, 3–8.
 DOI:10.1107/S2053273314026370
- 9. L. Z. Qiao, K. Lu, M. L. Qi, R. N. Fu, *J. Chromatogr. A.* **2013**, *1276*, 112–119. **DOI**:10.1016/j.chroma.2012.12.039
- (a) Q.Liu, J. H. Lin, J.Liu, W.Chen, Y. M. Cui, Acta chim. Slov. 2016, 63, 279–286.

- (b) Q. A. Peng, X. P. Tan, Y. D. Wang, S.H. Wang, Y. X. Jiang, Y. M. Cui, *Acta chim. Slov.* **2020,** *67*, 644–650;
- DOI:10.17344/acsi.2019.5650
- (c) S. S. Qian, X. L. Zhao, J. Wang, Z. L. You, *Acta chim. Slov.* **2015**, *62*, 828–833.
- (a) P. Zhang, S. J. Qin, M. L. Qi, R. N. Fu, J. Chromatogr. A.
 2014, 1334, 139–148. DOI:10.1016/j.chroma.2014.01.083
 (b) X. M. Shuai, Z. Q. Cai, X. Y. Zhao, Y. J. Chen, Q. Zhang, Z. W. Ma, J. J. Hu, T. Sun, S. Q. Hu, Chromatographia. 2021, 84, 325–333. DOI:10.1007/s10337-021-04018-x
 (c) T. Sun, B. Li, Y. Li, X. Y. Zhao, Q. Q. Song, X. X. Jiang, X.
 - M. Shuai, Y. Y. Li, Z. Q. Cai, S. Q. Hu, *Chromatographia*. **2019**, 82, 1697–1708. **DOI**:10.1007/s10337-019-03783-0

Povzetek

V prispevku opisujemo raziskave separacijskih lastnosti p-tert-butil(tetradeciloksi)calix[6] arena (C6A-C10-OH) kot stacionarne faze za plinsko kromatografijo (GC). Spojino smo karakterizirali z IR, 1 H NMR, 13 C NMR, MS in monokristalno rentgensko analizo. Kolona C6A-C10-OH ima dobre separacijske lastnosti za alifatske, aromatske in cis-trans-izomere. Omogoča številne molekularne interakcije za analite s širokim razponom polarnosti, vključno z disperzijskimi silami, vodikovo vezjo, π - π in dipol-dipol interakcijami. Delo ponuja eksperimentalno in teoretsko podlago za razvoj novih stacionarnih faz na osnovi calixarenov v GC analizi.

